Journal Club: Quasiparticle Poisoning in Superconducting Devices

Valla Fatemi

11/4/2016

Contents

1 Brief Intro to Superconductivity

BCS theory, electron-phonon interaction, superconducting gap, Josephson supercurrent.

2 Quasiparticles in SC

2.1 Early notes and simple calculation

Hints at this as early as 1962, Ginsberg experiment and Schrieffer and Ginsberg theory, where they calculated the quasiparticle recombination time due to phonons, and measured an upper limit. The measured "upper limit on the recombination time" was 1 OOM longer than the theoretical time.

At a given temperature, the equilibrium density of single quasi-particles at the gap edge is given by the distribution function

$$f \sim \frac{1}{1+\exp\left(\frac{\Delta}{kT}\right)} \sim \exp\left(-\frac{\Delta}{kT}\right) \tag{1}$$

For aluminum ($\Delta \sim 200\mu eV$) at 25 mK ($kT \sim 4\mu eV$) we have $\frac{\Delta}{kT} \sim 50$, the occupation is

$$f \sim e^{-50} \sim 10^{-22}. \tag{2}$$

The Density of states of Aluminum near the Fermi energy is about $0.4\frac{states}{eV \cdot f.u.}$, where one "formula unit" is a unit cell of volume ~$0.06nm^3$, so the DOS is ~$7\frac{states}{eVnm^3}$. To estimate the thermal number occupation of an island ~ 100nm on a side, we do the integral:

$$\begin{aligned}
2\int_{\Delta}^{\infty} DOS(E_F)\frac{E}{\sqrt{E^2-\Delta^2}}\exp\left(-\frac{E}{kT}\right)dE &= 2\cdot DOS(E_F)\int_{\Delta}^{\infty}\frac{E}{\sqrt{E^2-\Delta^2}}\exp\left(-\frac{E}{kT}\right)dE && (3)\\
&= 2DOS(E_F)\frac{1}{\Delta}\int_{\Delta}^{\infty}\frac{E}{\sqrt{\frac{E^2}{\Delta^2}-1}}\exp\left(-\frac{E}{kT}\right)dE && (4)\\
&= 2DOS(E_F)kT\int_{\Delta/kT}^{\infty}\frac{x}{\sqrt{x^2-\frac{\Delta^2}{k^2T^2}}}\exp\left(-x\right)dx && (5)\\
&\sim 2DOS(E_F)\Delta\sqrt{\frac{\pi kT}{2\Delta}}\exp\left(-\frac{\Delta}{kT}\right) && (6)\\
&\sim DOS(E_F)\sqrt{2\pi kT\Delta}\exp\left(-\frac{\Delta}{kT}\right) && (7)
\end{aligned}$$

Where $DOS(E_F) \sim 10^{28}\frac{states}{eV\cdot m^3}$ in aluminum, giving us about $\sim 100m^{-3}$ for aluminum at $50mK$, and many orders of magnitude smaller than that for $25mK$ and lower.

2.2 Measurements of QP density

A wide variety of experiments has consitently found that the number of quasiparticles far exceeds what is expected in equilibrium. This non-equilibrium population has yet to be explained, but is important for many applications of superconductivity, particularly as a limitation. As a result it is called "poisoning", since it causes problems but the source isn't necessarily known. This term was first coined in a 1994 paper by Devoret and collaborators (while he was still in France) studying a system similar to the one I will discuss. Today, I will largely outline a 2004 paper by Devoret (in Yale), and also the implications of a 2015 Nature Physics article by the Delft group. Here I will focus on the effects of quasiparticle poisoning on superconducting single-Cooper pair transistors (SCPTs). If we have time I will discuss implications for future Majorana devices.

Here are a few explicit measurements of the quasiparticle density in aluminum at low temperatures:

- Shaw et al (2009) estimate $10\mu m^{-3} \sim 10^{19}m^{-3}$ by looking at the kinetics of quasiparticle tunneling onto and off of a Cooper pair box.
- Saira et al (2012) get an upper bound of $n_{qp} < 0.033\mu m^{-3} \sim 3.3e16m^{-3}$ by measuring transition rates from superconducting leads onto a normal mental Coulomb island at the degeneracy point.
- Court, et al, (2008) find a saturation QP temperature of order $300mK$ without traps and $200mK$ with traps.

2.3 Models for QP poisoning

I have found two papers that attempt to theoretically model the nonequilibrium quasiparticle density given an unknown source of quasiparticle generation.

2.3.1 Martinis, et al. PRL 2009

Here the authors take advantage of how well understood aluminum is, and develop theory to show what the energy distribution of the quasiparticle density is in the case of only electron-phonon relaxation, in particular noting the electron-phonon scattering time is $\sim 400ns$. The idea here is that one excites a pair of quasiparticles at some energy $\gg \Delta$. Phonons then efficiently relax this high-energy pair down to energies near Δ. The recombination time to actually re

2.3.2 Bespalov, et al. PRL 2016

Here the authors utilize more advanced theory regarding how the density of states is modified by disorder, which induces real-space fluctuations in Δ. These fluctuations create bound-states and the authors derive several relevant sub-Δ energy scales. In the end, the model can reduce to the notion that QPs get trapped in random locations, and a simple "bursting bubbles" model can pictorialize their theory. Basically, imagine random QPs appear in random locations with a particular radius r_c determined by the gap fluctuations. If a QP appears and it's radius overlaps with an existing QP, then they annihiliate (likely emitting a phonon). If a QP appears without overlapping with anyother one, then it stays. Given a particular "generation rate" of QPs and QP radius, one can write down the non-equilibrium concentration according to the theory, and it is in general much much higher than the thermal one.

This paper doesn't seem to address the frequently cited diffusion length of QPs (many microns or even mms) and also the question of why quasiparticle traps can be effective. They claim trap depths of order 10^{-2} to 10^{-4} are reasonable, which means length-scales of order 4 to 9 coherence lengths, which is at most on the 10-micron scale for very clean aluminum, and much shorter otherwise.

2.3.3 Possible Nonequilibrium Energy Sources

- Cosmic rays
- Thermal leakage from 4K and 1K stages of the fridge
- Slow heat release from amorphous SiO2, poly-xtal Al, and Teflon at low temperatures

2.4 Why is QP poisoning bad?

Qubits Any time you need charge # or parity to be a stable quantum number of your system, poisoning can be a problem. Also, when QP hop across Josephson junctions this can couple to the flux-basis of flux-based qubits. These devices include:

1. Cooper pair box: takes you out of the Hilbert space when a QP goes on the island
2. Transmon: T_2: charge is no longer a good quantum number here, charge fluctuations can still matter for dephasing.
3. Fluxonium: T_1: when a QP hops across the JJ and loses/gains energy resonant with qubit frequency $\hbar\omega_q$ it can excite/relax the qubit state.
4. Majorana-based quantum computation: parity must be stable!

Other Devices

1. Kinetic Inductance Detector: the kinetic inductance of a superconductor depends on the number of Cooper pairs, and the detector measures the resonant frequency of an LC circuit based on this inductance. The contrast comes from a change in L when Cooper pairs are broken by an incident photon, and a non-equilibrium density of QPs will worsen said contrast.

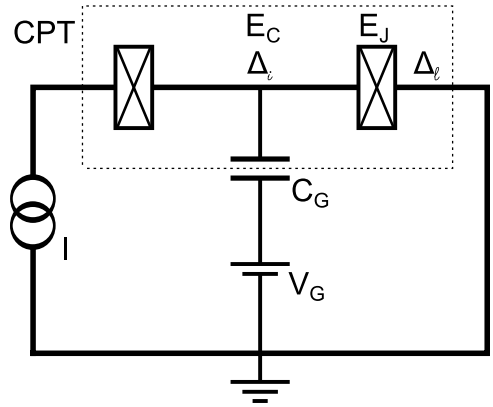

Figure 1: Circuit diagram of a typical experimental setup of a SCPT. The SCPT itself is inside the dotted line box.

2. SQUID amplifiers: hot quasiparticles contribute to noise in the system.
3. Energy decay in superconducting resonators

3 Set up of SCPT

See circuit in Figure 1.

3.1 Energy Scales

The discussion here regards the case of a Cooper pair box, which consists of a superconducting island with charging energy $E_C \sim e^2/2C$, connected by tunnel Josephson junctions (JJs) to superconducting leads. The island and leads may have different superconducting gaps Δ_I, Δ_L. Finally, the nature of the Josephson junctions is that the system will have a third energy scale called the Josephson energy EJ. If we choose to say that supercurrent goes like

$$I_s = I_c \sin\phi \tag{8}$$

Energy of a JJ goes as the work done to accumulate a certain phase:

$$U = \int_0^t I_s V dt = \frac{\phi_0}{2\pi}\int I_s \frac{d\phi}{dt} dt = \frac{\phi_0 I_c}{2\pi}\int \sin\phi d\phi \tag{9}$$

$$U = E_J\left(1-\cos\phi\right) \tag{10}$$

$$E_J = \frac{\phi_0}{2\pi} I_c \tag{11}$$

which is similar to having a characteristic energy scale for the nonlinear inductor that is the JJ itself.

So we have three characteristic energy scales:

$$E_J \rightarrow \text{energy scale of JJ, energy scale of hybridization between states } N \text{ and } N+2 \tag{12}$$

$$E_C \rightarrow \text{energy scale of adding charge to the island} \tag{13}$$

$$\Delta_{I,L} \rightarrow \text{energy scale of adding a quasiparticle, offset energy difference between even/odd states} \tag{14}$$

The fact that $E_J > 0$ tells us that the tunnel coupling is strong.

3.2 Simple Model

Here we assume a hamiltonian in the $\Delta \gg E_C$ case. We consider that the good quantum numbers of the system are the charge of the island n and the total phase difference across the island and its JJs ϕ. If we take as basis

states those with charge 0 and 2 we can write a hamiltonian

$$H = \begin{pmatrix} E_C(0-n_g)^2 & -E_J\cos\frac{\phi}{2} \\ -E_J\cos\frac{\phi}{2} & E_C(2-n_g)^2 \end{pmatrix} \tag{15}$$

which is easily diagonalizable by using Pauli matrices. Define the following parameters:

$$M(n_g) = E_C(n_g^2 - 2n_g + 2) \tag{16}$$

$$D(n_g) = 2E_C(1-n_g) \tag{17}$$

$$J(\phi) = E_J\cos\frac{\phi}{2} \tag{18}$$

so we can re-write the hamiltonian as

$$H = M(n_g) + D(n_g)\sigma_z + J(\phi)\sigma_x \tag{19}$$

Here, by analogy to Zeeman effect, we can see that the charge basis states are still good quantum numbers if $E_J = 0$ or if $\phi = \pi$.

This Hamiltonian is easily diagonalizable:

$$\varepsilon_{a,b} = M(n_g) \pm \sqrt{D(n_g)^2 + J(\phi)^2} \tag{20}$$

with eigenstates defined as following, also defining $2\alpha = \arctan\left(\frac{J}{D}\right)$,

$$\psi_- = \cos\alpha\,|0\rangle + \sin\alpha\,|2\rangle \tag{21}$$

$$\psi_+ = \sin\alpha\,|0\rangle - \cos\alpha\,|2\rangle \tag{22}$$

We can again see that for $J = 0$, $\alpha = 0$ so the charge states are good eigenstates. When $D = 0$ and $J > 0$, $\alpha = \frac{\pi}{4}$, so the eigenstates are exactly equal superpositions of 0 and 2.

3.3 Full Energy of the SCPT States vs Gate

A better energy spectrum requires solving the hamiltonian for three charge states, since at (for example) $n_g = 0$, the $n = 0$ state couples equally to $n = \pm 2$. This will generate all the model we see following this point.

Let us start with the totally trivial case: no superconductivity whatsoever. Here, we have no pairing within the island to split the even/odd degeneracy, but the Coulomb energy still causes charge to change in a quantized fashion. Without Josephson coupling, when two states that differ by two charges are degenerate, they remain degenerate and we find a resonance in normal transport. This is the zero bias conductance peak of a normal Coulomb island. See Figure 2(a) for the energy diagram of this.

Now let us imagine that there is no Josephson coupling, but we turn on a superconducing pairing energy Δ on the island. This means that there is an additional energy cost of Δ to add a single charge to the island. As a result, the free energy diagram looks like in Figures 2(b) and (c), for the case of $\Delta < E_C$ and $\Delta > E_C$, respectively. We see that in the first case, both even and odd states are still allowed, but the odd states have a narrower range of gate voltage for which they are stable. For the second case, the pairing gap overwhelms the charging energy, resulting in charge oscillations of $2e$ rather than $1e$.

Now let us add Josephson coupling. We could imagine a fictitious situation in which there is a finite Josephson coupling but zero superconductivity on the island itself. Here we would see that when two states differing in charge by $2e$ cross, they are hybridized by the Josephson coupling and therefore anticross. See Figure 2(d). However, this is not physical since we need superconductivity on the island to have Josephson coupling.

So, we can imagine the case of having a Josephson coupling energy E_J as well as the pairing energy Δ, resulting in the energy diagrams in Figures 2(e) and (f), which can be seen to be a a combination of (d) with (b) and (c) respectively. The behavior of the ground state of the island as a function of gate charge is not changed very much, but we will see that the cases $\Delta < E_C$ and $\Delta > E_C$ will have a large effect on the critical current in the system. An important thing to note is that the even and odd subspaces are uncoupled and behave exactly the same, except that the odd subspace is shifted by $1e$ in gate charge and $+\Delta$ in energy.

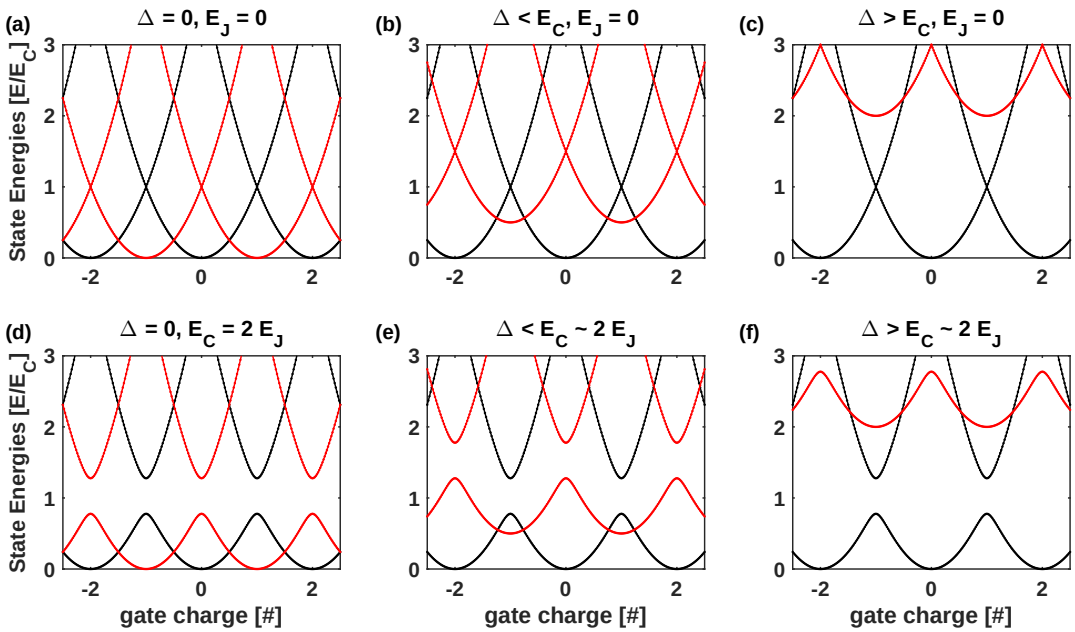

Figure 2: Energy of SCPT states vs gate charge under different cases of energy scales. Black = even states, red = odd states.

3.4 Supercurrent of an even-only SCPT, $\Delta \gg E_C$

We will first look at the supercurrent for the cases of Figure 2(f), where we would nominally only have to consider the even-states. We look only at the ground state energy, and observe it's behavior as a function of phase difference (Figure 3(a)) as well as gate charge (reproduced again in Figure 3(b), also at different phases). Just as in a normal Josephson junction, the energy of the system is raised for phase difference $\phi \sim \pi$ compared to $\phi \sim 0$. This can be considered as the energy stored in the intrinsic inductance of the Josephson junction, as described in Section 3.1.

The current at a given phase is given by the phase-derivative of the ground state energy:

$$I_s = \frac{\phi_0}{2e}\frac{dE_{gs}}{d\phi} \tag{23}$$

where $\phi_0 = h/2e$ is the quantum of flux. The critical current I_c is merely the maximum of this quantity, which we can calculate for each value of gate charge, to obtain Figure 3(c). We find that it is sharply peaked near the resonance between N and $N+2$ charges on the island, as we might expect. Note that the odd subpace, would have an identical behavior of its I_c, except shifted by $1e$ in the gate charge map.

3.5 Supercurrent of an even and odd SCPT $\Delta < E_C$

Recall again that $I_c^{odd}(n_g) = I_c^{even}(n_g+1)$, as shown in Figures 4(c-e). There we see different cases for the ratio Δ/E_C, where $E_J = 0.7E_C$. When $\Delta \gtrsim E_C$, we find that the odd states are never energetically favorable, resulting in strictly $2e$-periodic oscillations in the occupation and critical current. But when $\Delta < E_C$, there are gate voltages at which the odd state is energetically favorable, resulting in sudden changes in the critical current – where I_C was previously a maximum, it suddently dips into a minimum! It could also be described as the peak bifurcating into two, smaller peaks. When $\Delta \ll E_C$, the system is nearly $1e$-periodic, and the oscillations in I_C are no longer sharply peaked. See Joyez, et al. PRL 1994 for experimental realization of the double-peaked structure shown in the figure.

3.6 Experimental Reality

The reality of life turns out to be that even in the case where $\Delta \gg E_C$, one can have $1e$-periodic supercurrent! How is this possible? Well, first let's see if this is possible in equilibrium. We can take the case of the far-right

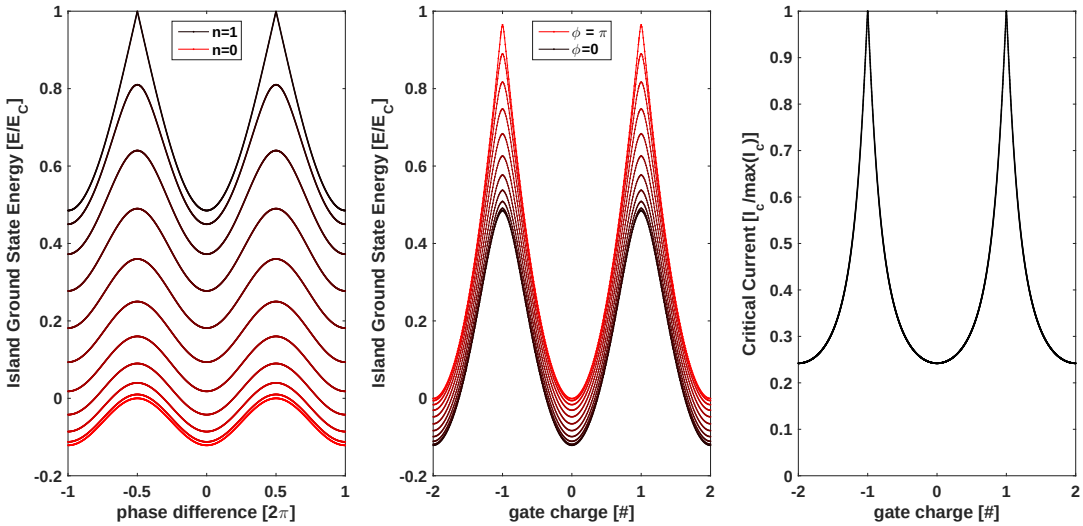

Figure 3: The ground state energy of the even-only island as a function of phase difference and gate charge. The maximum of the phase-derivative of this energy gives the critical current. Here $E_C = 2E_J$

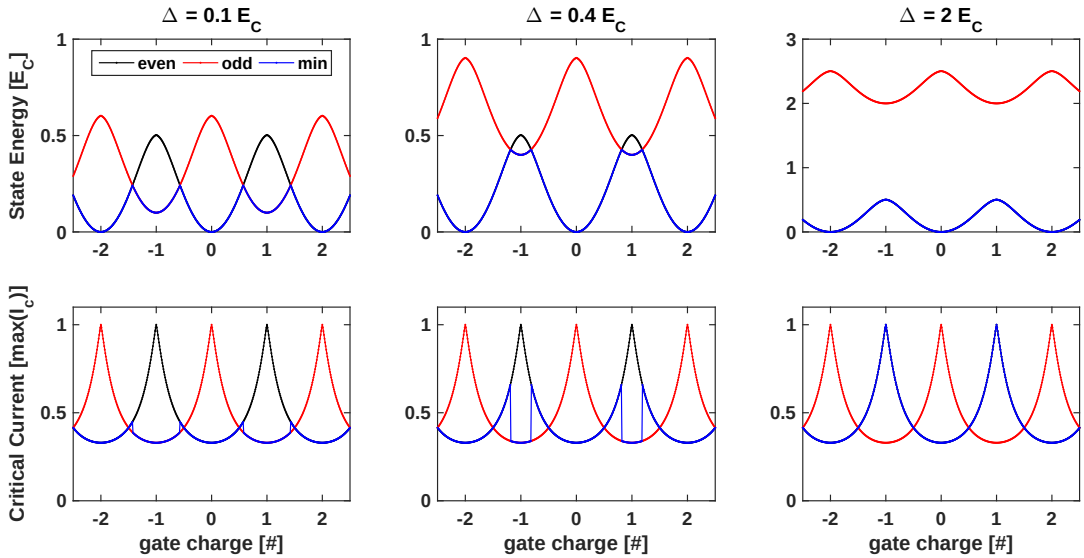

Figure 4: Energy states and critical current for different cases of Δ/E_C. For all scenarios, $E_J = 0.7E_C$, which is typical.

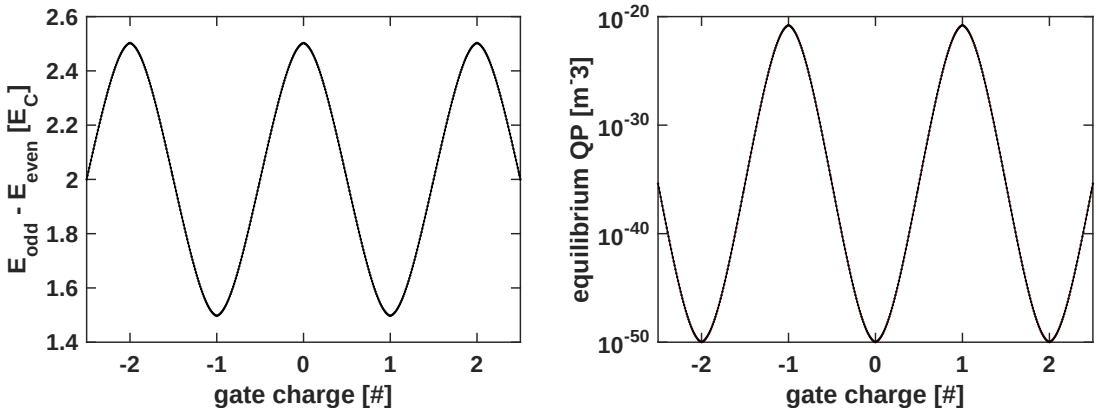

Figure 5: sss

panel of Figure 4 as a typical case (see Aumentado, PRL 2004). From this, we can plot the energy difference between the even and the odd state as a function of gate charge, and then calculate the equilibrium quasiparticle density based on the temperature of the measurement $T \sim 20mK$ so $kT \sim 1.7\mu eV$. We see this in Figure 5, where the energy difference is plotted vs gate charge #, in units of E_C. For the experiment at hand, $E_C = 115\mu eV$, $\Delta \sim 2E_C$, and $E_J \sim 0.7E_J$, which gives us this model calculation. From this we can calculate the equilibrium density of quasiparticles as per 3.1, and find that even if the island were a 1 meter cube then the density of quasiparticles is vansihingly small, let alone for an island of order $100nm$ in scale.

So this suggests that for typical device parameters, only $2e$-periodic oscillations should be found. And yet, many scientists reliably find $1e$-periodic behavior in many junctions fabricated in a similar way. This is a strong indication for a non-equilibrium density of quasiparticles, e.g. a "hot" quasiparticle distribiution compard to the lattice temperature. Now, let's dig into what they find in the experiment.

3.7 Why are these devices useful?

Early superconducting qubits were made out of half of a CPT, e.g. with just one JJ. Here there is no phase dependence, but still the induced gap of order E_J between N and $N+2$, and this was the logical subspace of the qubit. This was called the charge qubit, but was unfortunately highly susceptible to (a) charge noise and (b) parity jumps via quasiparticle poisoning, which we shall discuss shortly.

The CPT itself was eventually implemented as an important component in the "quantronium" qubit.

More generally, it is theoretically and experimentally an easily understood system that can be used to test ideas, etc.

4 Aumentado, et al. PRL 2004

4.1 Introduction and Basic Experimental Result

Here they make a device with circuit diagram exactly as shown in Figure 1, and the key different is the addition of another parameter: a different superconducting gap energy in the leads Δ_L vs the island Δ_I. Both gaps are larger than all other energy scales, e.g. $\Delta_{I,L} > E_C, E_J$, and the charging energy is only slightly larger than the Josephon energy. See Table 1 for details on all energy scales.

As per sections 3.5-3.6, in equilibrium one would expect $2e$-periodic oscillations for both devices. However, as we see in Figure 6, the switching current in the Type L device has $1e$-periodic oscillations whereas the Type H device has $2e$-periodic oscillations. The existence of $1e$-periodic oscillations is only possible due to a non-equilibrium density of quasiparticles, for such similar devices, how is it possible for the other one to have $2e$-periodic oscillations?

This experiment was cleverly designed with a spatial profile of the superconducting gap, e.g. an energy landscape for excited quasiparticles. The Type L devices is like a quasiparticle well, whereas the Type H device is a quasiparticle barrier, e.g. the leads serve as a sort of "quasiparticle well". The energy difference between the island and leads is substantial: $|\Delta_L - \Delta_I| \sim 40\mu eV \sim 15kT$, which will play the crucial role here.

	Type L Device	Type H Device
Δ_I	205	246
Δ_L	246	205
E_J	78	82
E_C	115	115
kT	2.2	2.2

Table 1: Energy scales of this experiment, all in μeV.

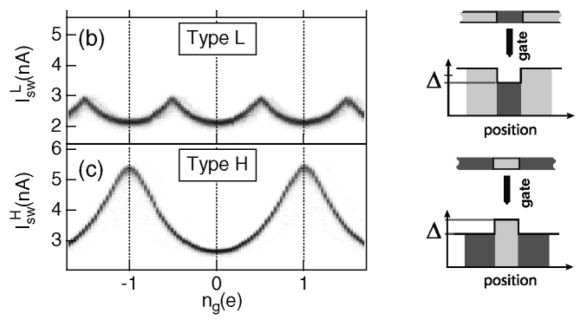

Figure 6: Left: Switching current as a function of gate charge for the two types of devices. Right: schematic of the change in the quasiparticle gap Δ as a function of position.

4.2 Model

To explain this behavior, the authors used a three-state model to understand what is going on, as shown in Figure 7. The ground state is the 0 state, with no quasiparticles anywhere. We assign this state the energy

$$E_0 = E^{n=0}_{C-J}(n_g, \phi) \tag{24}$$

. The next state "l" has a single quasiparticle in one of the two leads, which has the same energy as the 0 state shifted by the superconducting gap in the leads:

$$E_l = \Delta_l + E^{n=0}_{C-J}(n_g, \phi) \tag{25}$$

$$E_l - E_0 = \Delta_l \tag{26}$$

. Note that this means that the energy difference between 0 and l is fixed by the superconducting gap: $E_l - E_0 = E_{l0} = \Delta_l$. The final state is the "poisoned" state E_i, with a quasiparticle on the island. This state has an energy offset of the island superconducting gap Δ_i and the phase dependence of the odd-parity state. In the following estimate, I consider $n_g \in \{0, 1\}$.

$$E_i = \Delta_i + E^{n=1}_{C-J}(n_g, \phi) \tag{27}$$

$$E_i - E_l = \Delta_i - \Delta_l + E^{n=1}_{C-J}(n_g, \phi) - E^{n=0}_{C-J}(n_g, \phi) \tag{28}$$

$$= \delta\Delta + E_C(2n_g - 1) - \sqrt{4E_C^2 n_g^2 + E_J^2 \cos^2\frac{\phi}{2}} + \sqrt{4E_C^2(1-n_g)^2 + E_J^2\cos^2\frac{\phi}{2}} \tag{29}$$

$$E_i - E_l|_{\phi=0} = \delta\Delta + E_C(2n_g - 1) - \sqrt{4E_C^2 n_g^2 + E_J^2} + \sqrt{4E_C^2(1-n_g)^2 + E_J^2} \tag{30}$$

We can evaluate this particularly at the extrema: $n_g = 0, 1$:

$$E_i - E_l|_{\phi=0, n_g=0} = \delta\Delta - E_C + E_J + \sqrt{4E_C^2 + E_J^2} \tag{31}$$

$$E_i - E_l|_{\phi=0, n_g=1} = \delta\Delta - \sqrt{4E_C^2 + E_J^2} + E_C + E_J \tag{32}$$

if we make the approximation $E_C \approx E_J$, then :

$$E_i - E_l|_{\phi=0, n_g=0} \approx \delta\Delta + \sqrt{5}E_J \tag{33}$$

$$E_i - E_l|_{\phi=0, n_g=1} \approx \delta\Delta - \left(\sqrt{5} - 2\right) E_J \tag{34}$$

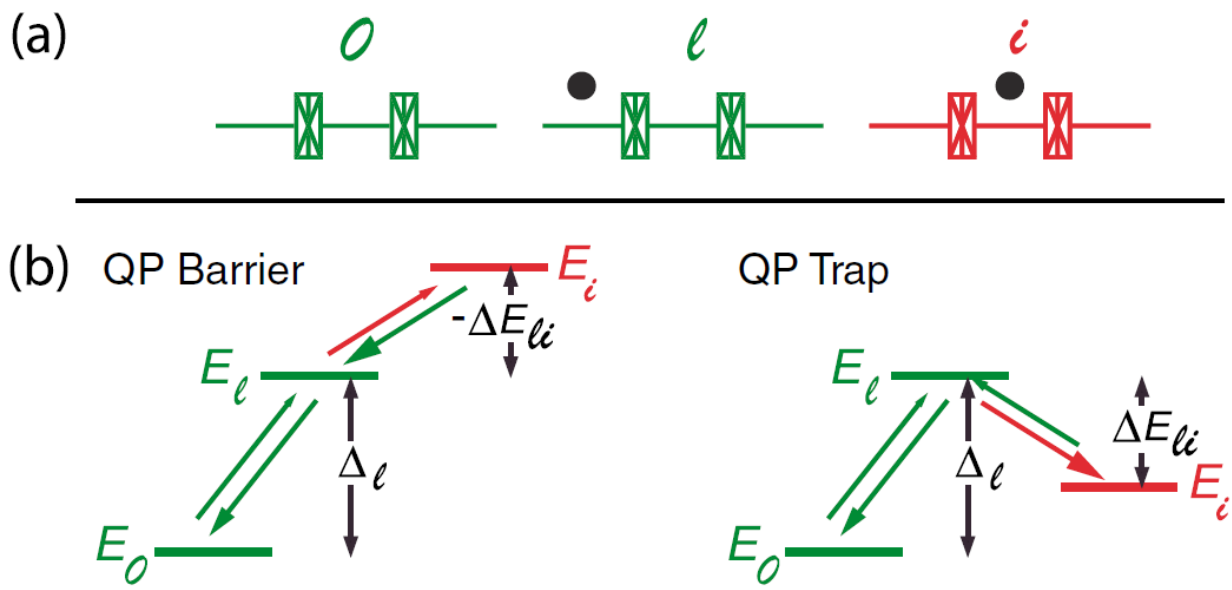

Figure 7: Three-state model by Aumentado. (a) left: no quasiparticles, middle: one quasiparticle in a lead, right: one quasiparticle on the island. (b) Energy diagram showing the relative difference between the three states for the two qualitatively different scenarios.

So in this approximation, whenever $\frac{\delta\Delta}{E_J} < \left(\sqrt{5}-2\right)$, then even having a QP barrier $\delta\Delta > 0$ is not sufficient for blocking QP entry for arbitrary gate charge. There is also a phase dependence to this, of course.

4.3 Parity Fluctuation Rate

The authors estimate a parity lifetime of order $10\mu s$. Let's see how they do that. The way that they estimate the critical current in this measurement is actually to measure the current at which the system "switches" into a finite voltage state. This switching current depends only on the parity of the island (not the leads). There are basically two limiting scenarios: slow and fast ramping of the current.

1. Infinitely slow ramp: If there is *any* probability that the island may have a quasiparticle on it, then an infinitely slow ramping rate will ultimately find the lowest possible critical current since the island will sample both possible states during the ramp. This scheme should always result in $1e$-periodic switching current.

2. Infinitely fast ramp: If the current is ramped up faster than the parity lifetime of the island, then you will sample the instantaneous switching current of the island in that moment. Doing many of these ramps and getting a histogram of the switching current should give a good idea of the overall probability of being in either the even or odd state. You can estimate whether you are approaching this regime by checking the following relationship:

$$\tau_{ramp} < \frac{\left|I_{sw}^{even} - I_{sw}^{odd}\right|}{\dot{I}_{ramp}} \tag{35}$$

Finding the transition between these two limits gives an estimate of the parity lifetime. For Figure 6, the ramp rate was $\dot{I}_{ramp} = 1\mu A/s$, and nearly $1e$ oscillations were found in the QP trap device, suggesting the ramp rate is slow enough to always sample the lowest critical current. By increasing the ramp rate to $\dot{I}_{ramp} = 100\mu A/s$ they start seeing datapoints higher than the minimal critical current, as shown in Figure8. This suggests that they are now ramping fast enough to preserve the parity sometimes. By checking the ramp time against the difference in the even and odd critical currents, they estimate the $\sim 10\mu s$ parity lifetime for the quasiparticle trap device.

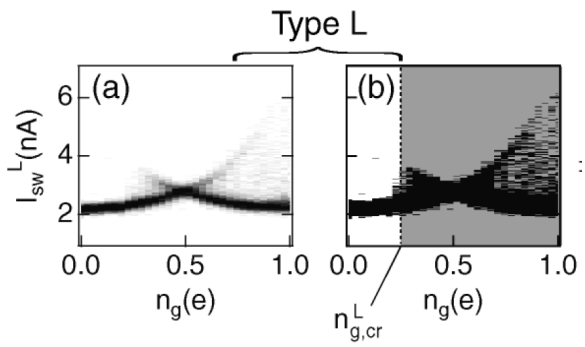

Figure 8: Histogram of switching current of the quasiparticle trap device for the faster ramp rate of $\dot{I}_{ramp} \sim 100\mu A/s$.

There is no cited parity lifetime for the QP barrier device, although there are a few counts of switching below the I_{sw}^{even}, suggesting they are on the verge of it. By using the same relationship as above, we can estimate that $\tau_p^H \sim 1ms$. Quite long already!

So this result pointed to a clear two-step path forward for obtaining long quasiparticle lifetimes for these types of devices:

1. Ensure the device is in a "QP barrier" formation, with island superconducting gap much larger than the lead superconducting gap: $\Delta_i \gg \Delta_l$
2. Institute normal-metal quasiparticle traps, which were used "blindly" by experimentalists prior to the Aumentado paper to obtain $2e$-periodic devices. See Joyez, et al. PRL 1994

This path forward was implemented in the next paper we will inspect.

5 Woerkom, et al. Nat. Phys. 2015

More recently, a headline article was published showing parity lifetimes of order 1 minute in an updated Cooper-pair transistor architecture, utilizing a NbTiN island. This device will have a similar QP-barrier type structure as from the Aumentado paper but comes with a materials/nanofabrication breakthrough in using NbTiN as the superconducting island. Table # compares the two papers, where we make sure to compare apples to apples by using Device "N" from the Woerkom paper that does NOT have any normal-metal QP traps near the device. We see that increasing the island superconducting gap by about a factor of 10 and reducing the temperature by about a factor of two results in an increase in the parity lifetime by...not even an order of magnitude. Why?

The authors claim that the limiting problem here is supposedly that NbTiN has a large sub-gap single-particle DOS, so that it is not strictly true that the "large" Δ_i is a huge benefit. This is termed a phenomenological Dynes parameter, which refers to the insertion of a complex energy to the superconducting density of states $E \to E - i\Gamma$, where Γ represents a broadening of the superconducting DOS due to the finite lifetime of the quasiparticles. They estimate that the sub-gap DOS is ~ 10^{-2} to 10^{-3} of the normal-state DOS, which comes from unknown origin. Presumably this substantial sub-gap DOS results in not such a huge energy barrier for single quasiparticles, making it easy for quasiparticles in the leads to hop onto the island. Essentially this is just measuring yet again that aluminum leads appear to have a large nonequilibrium QP density, and despite the large theoretical superconductig gap of NbTiN, there are confounding material parameters that disallow ideal behavior of the QP barrier structure.

5.1 Shunted device behavior

However, their shunted devices display *substantially* longer quasiparticle lifetimes, longer than observed for any aluminum-based device. Even better, device S2 appears to show no saturation in the lifetime down to the lowest fridge temperatures. Fitting to a model finds an activated energy scale of order $20\mu eV$. They claim that this is energy scale is that of the even-odd energy difference at $n_g = 1$. If the NbTiN island had zero DOS at zero energy, then this would not be the case. But the finite sub-gap density of states results in *some* weight remaining for

	Aumentado, QP barrier	Woerkom, Device N	Woerkom, Devices S1, S2
Δ_I	246	1100	1100
Δ_L	205	200	200
E_J	82	~40	~40
E_C	115	50	50
kT	2.2	1.0	1.0
τ_p	~$1ms$	$10ms$	0.8 and 60 s
Notes	"inside rf-tight copper box"	"single copper rf shield with infrared absorbing paint"	"double copper rf shield with infrared absorbing paint"

Table 2: Comparison of device parameters for the QP barrier device from the Aumentado paper and the NbTiN device from the Woerkom paper. All energy scales in μeV.

odd-parity states not shifted by the superconducting gap. This is their proposal for the *energy scale*, which only controls the slope of the temperature dependence. The absolute magnitude of the lifetime also depends on the sub-gap DOS which comes as a pre-factor to the temperature dependence.

Would there be ways to improve this energy scale? Larger E_C and smaller E_J could help.

5.2 Calculation of tunneling rate

The zero-bias conductance of a system we can find a quasiparticle tunneling rate based on (a) the density of quasiparticles in the leads, (b) the tunneling conductance, and (c) the sub-gap density of states of the island:

$$\tau_p^{-1} = \frac{G_N}{e^2 \rho_{Al}} \frac{\rho_{subgap}}{\rho_{NbTiN}} n_{qp} \tag{36}$$

where the normal state tunneling condutance is proportional to the DOS in both island and lead:

$$G_N \sim \rho_{Al} \rho_{NbTiN} \tag{37}$$

and the non-equilibrium particle density is proportional to the aluminum density of states, giving us a scaling

$$\tau_p^{-1} \sim \rho_{subgap} \rho_{Al} \tag{38}$$

which is what we expect.

In particular, the zero-bias conductance (assuming very low T and constat tunneling matrix element) is

$$\frac{d}{dV} I = \frac{4\pi e}{\hbar} T \left[\frac{d}{dV} \int_0^{eV} \rho_{Al}(E_F - eV + \varepsilon) \rho_{NbTiN}(E_F + \varepsilon) d\varepsilon \right]_{V=0} \tag{39}$$

$$G_N = \frac{4\pi e}{\hbar} T \rho_{Al}(E_F) \rho_{NbTiN}(E_F) \tag{40}$$

so the tunneling rate they ascribe is basically a way of normalzing to a measurable quantity that avoids needing to think about tunneling matrix element T. This way they can try to fit the data the non-equilibrium QP temperature, where we use equation (7) for n_{qp}:

$$\tau_p^{-1} = \frac{4\pi}{e\hbar} T \rho_{Al} \rho_{subgap} \sqrt{2\pi k T \Delta_{Al}} \exp\left(-\frac{\Delta_{Al}}{kT}\right) \tag{41}$$

$$= \frac{G_N}{e^2} \frac{\rho_{subgap}}{\rho_{NbTiN}} \sqrt{2\pi k T \Delta_{Al}} \exp\left(-\frac{\Delta_{Al}}{kT}\right) \tag{42}$$

They use this thermal activation scheme to fit the data in various regimes. They find that above $T \sim 120mK$ the fitting parameter Δ_{Al} is of order $200\mu eV$, suggesting equilibrium quasiparticle densities above those temperatures, which is consistent with the history of the field.

5.3 1 minute lifetimes

Below that temperature, devices S1 and S2 show a different activation gap of $\Delta^* \sim 20\mu eV$, which they claim is the energy barrier to the other-parity state if there is no superconducting gap for the odd-parity state. Essentially this is the minimum comes from the fact that they island has a not-insignificant sub-gap DOS that is not gapped by superconductivity.

This is an interesting interpretation, but weird. An even state does not simply get thermally activated into an odd state. Charge must move around. Let's think about mechanisms:

- The scheme suggested by Aumentado cannot produce this energy scale. Δ_{island} so overwhelms every other energy scale.
- Let's say some non-equilibrium source breaks a Cooper pair on the island. the charge state stays the same, but the states live up at Δ_i. It is then energetically favorable for them to tunnel into the aluminum since they can then relax to Δ_l. What is perhaps likely is that they would like to tunnel elastically into the aluminum lead, but then the energy of the island must be raised by a *minimum* of $\delta E \sim E_C - E_J/2 \sim 20\mu eV$, as noted in the text.
- Perhaps equivalently, a QP can just tunnel elastically from the Al lead onto the island, but must overcome the same energy barrier. Given such a large ρ_{subgap}, it is surprising to me that the QP does not undergo the "fully elastic" hop in which it drops its single-particle energy by δE to compensate for the increased Coulomb energy.

5.4 Effect of Magnetic Field

If a magnetic field induces vortices in the leads, then there will exist normal metal islands there that will tend to suck up QPs and keep them (a) far away from the crucial device area and (b) at low energy compared to Δ.

If, on the flip side, a vortex is induced inside the CPT, then the sub-gap density of states becomes larger, resulting in an increased QP switching time.

See Figure 4 from the paper for experimental demonstration of this.

6 Implications for Majorana Devices

So the final upshot here is: what implications does this have for Majorna islands? In this case, there is explicitly a finite DOS at zero energy (which is localized at the ends of the island in real space). These Majorana modes can be occupied (odd parity) or unoccupied (even parity). Therefore, the superconducting gap no longer gaps out odd-parity states, and the island is perpetually in the "QP well" scenario of the Aumentado paper. The key difference here is that the QP DOS is no longer represented by the bulk metal DOS multiplied by the gap function, but instead just a single state, regardless of the volume of the system. This should substantially reduce the ability for QP to tunnel onto the island.

If we imagine an ideal island superconductor with no subgap DOS other than the Majorana itself, what could we expect under similar circumstances as the Woerkom paper, or can we improve? There are a few intriguing things.

1. Now instead of ρ_{subgap} we have just a single state, which should improve things substantially. For example, given Dynes parameter of 10^{-2}, the number of sub-gap states available inside the aluminum gap energy window is of order 1000. So if we reduce to just 1, then the parity lifetime should improve by that much to a sort of "ideal" value given by the mere presence of a Majorana itself (and the nonequilibrium population in the leads).
2. Second, one could design the EM environment to suppress photon DOS for energies of order Δ_l so that quasiparticles can't hop from the leads onto the Majorana state (if photon emission is the way energy is lost in the transition).
3. Issues of magnetic field – the lifetime drops dramatically when a vortex can penetrate into the system. So the smaller the island the better in this case. But with a charging energy the two Majorana states are not denerate anyway, so one needs a long sample, which results in easy admission of a flux quantum.

7 Appendices

7.1 Dynes Parameter

An ideal BCS superconductor has a modification to the density of states that looks like

$$\rho_{BCS} = \mathrm{Re}\frac{E}{\sqrt{E^2 - \Delta^2}} \tag{43}$$

which is zere for $E < \Delta$. This is never observed, especially at high temperatures. Dynes (Dynes et al, PRL 1978) introduced a modified form, which is predicted to be "ok" near the gap edge:

$$\rho_{Dynes} = \mathrm{Re}\frac{E + i\Gamma}{\sqrt{(E + i\Gamma)^2 - \Delta^2}} \tag{44}$$

which is essentially introducing a lifetime to the quasiparticles, giving a broadening to the DOS. At low energy DOS saturates at a constant: $\rho(0) = \frac{\Gamma}{\sqrt{\Gamma^2+\Delta^2}}$. The physical validity of this formula has been disputed, but it is widely used to approximate the sub-gap DOS. One formula that is argued to be better, and more accurate microscopically (and fits data better) is the following (Mitrovic, et al. J Phys. Cond. Mat. 2008):

$$\rho_{Mitrovic} = \mathrm{Re}\frac{E}{\sqrt{E^2 - (\Delta - i\delta)^2}} \tag{45}$$

which gives a low-energy value of $\rho(E \ll \Delta) \approx \frac{E\delta}{\Delta^2+\delta^2}$.

Either way, such broadening of the BCS density of states results in a finite DOS at low energies, so that the odd-parity state may not be "fully" gapped out.

Naturally, reducing the sub-gap density of states would be a prime target for improving the parity lifetime even further. For comparison, upper bounds of the "Dynes parameter" for good aluminum films are of order 10^{-7}, which is roughly the ratio of the subgap DOS to the normal state DOS for that system. The NbTiN case has a value of order 10^{-2} to 10^{-3}, so there is substantial room for improvement.

7.2 Quasiparticle Density Sanity check: standard semiconductor

Note that Silicon has a similar $\frac{E_g}{kT} \sim 22$ at room temperature. Here the integral is a bit different:

$$6V\int_{E_g}^{\infty} DOS(E - E_c)\exp\left(-\frac{E}{kT}\right)dE = \frac{48\sqrt{2}\pi}{h^3}m_{eff}^{1.5}\int_{E_g}^{\infty}\sqrt{E - E_g}\exp\left(-\frac{E}{kT}\right)dE \tag{46}$$

$$= \frac{48\sqrt{2}\pi}{h^3}m_{eff}^{1.5}e^{-\frac{E_g}{kT}}\sqrt{k^3T^3}\int_0^{\infty}\sqrt{x}\exp(-x)\,dx \tag{47}$$

$$= 24\sqrt{2\pi^3}\sqrt{\frac{k^3T^3m_{eff}^3}{\hbar^6}}e^{-\frac{E_g}{kT}} \tag{48}$$

The factor out front is 6 to account for spin and valley degeneracy, only looking at the conduction band. For $T = 300K$, $m_{eff} \sim 1m_e$, and $E_g \sim 1.1eV/2$ this expression gives us a 3D electron density of $4.2 \times 10^{10}cm^{-3}$, which looks correct after doing a quick google search to verify.

7.3 Superconductivity in thin-film aluminum

Bulk, single-crystalline aluminum is a type-I superconductor, with a coherence length $\xi \sim 1600nm$ and a London penetration depth $\lambda \sim 16nm$. However, thin-film, or highly granular films of aluminum. the coherence length can shorten dramatically and the London penetration depth can become much longer, turning it into a type-II superconductor. This is why vortices can form in the leads of various CPT devices, such as in Woerkom, et al, resulting in an increase in the parity lifetime due to increased QP trapping in the normal cores.